Ecotoxicology and Environmental Safety 123 (2016) 81–88

Contents lists available at ScienceDirect

Ecotoxicology and Environmental Safety

journal homepage: www.elsevier.com/locate/ecoenv

Phytotoxicity of ionic, micro- and nano-sized iron in three plant species

G. Libralato [a,b,*], A. Costa Devoti [a,b,c], M. Zanella [b], E. Sabbioni [b,d,e], I. Mičetić [b], L. Manodori [b], A. Pigozzo [b], S. Manenti [d], F. Groppi [d], A. Volpi Ghirardini [a]

[a] Department of Environmental Sciences, Informatics and Statistics, University Ca' Foscari Venice, Campo della Celestia, Castello 2737/B, I-30122 Venice, Italy
[b] ECSIN-European Center for the Sustainable Impact of Nanotechnology, Veneto Nanotech S.C.p.A., Viale Porta Adige 45, I-45100 Rovigo, Italy
[c] In.T.Ec. s.r.l., Via Romea, 8, 30034 Mira, Italy
[d] LASA, Universita' degli Studi di Milano and INFN-Milano, via F.lli Cervi 201, I-20090 Segrate, Milan, Italy
[e] CeSI, Aging Research Center, "G. d'Annunzio" University Foundation, Via Colle dell'Ara, I-66100 Chieti, Italy

ARTICLE INFO

Article history:
Received 1 April 2015
Received in revised form
17 May 2015
Accepted 21 July 2015
Available online 29 July 2015

Keywords:
Lepidium
Sinapis
Sorghum
Nano-zerovalent iron
Nanoecotoxicology
Phytotoxicity

ABSTRACT

Potential environmental impacts of engineered nanoparticles (ENPs) can be understood taking into consideration phytotoxicity. We reported on the effects of ionic ($FeCl_3$), micro- and nano-sized zerovalent iron (nZVI) about the development of three macrophytes: *Lepidium sativum*, *Sinapis alba* and *Sorghum saccharatum*. Four toxicity indicators (seed germination, seedling elongation, germination index and biomass) were assessed following exposure to each iron concentration interval: 1.29–1570 mg/L ($FeCl_3$), 1.71–10.78 mg/L (micro-sized iron) and 4.81–33,560 mg/L (nano-iron). Exposure effects were also observed by optical and transmission electron microscopy. Results showed that no significant phytotoxicity effects could be detected for both micro- and nano-sized zerovalent irons, including field nanoremediation concentrations. Biostimulation effects such as an increased seedling length and biomass production were detected at the highest exposure concentrations. Ionic iron showed slight toxicity effects only at 1570 mg/L and, therefore, no median effect concentrations were determined. By microscopy, ENPs were not found in palisade cells or xylem. Apparently, aggregates of nZVI were found inside *S. alba* and *S. saccharatum*, although false positives during sample preparation cannot be excluded. Macroscopically, black spots and coatings were detected on roots of all species especially at the most concentrated treatments.

© 2015 Elsevier Inc. All rights reserved.

1. Introduction

Engineered nanomaterials (ENMs) are highly preferred for a broad spectrum of applications due to their unique properties. Engineered nanoparticles (ENPs) have a promising use in many areas including catalysis, optics, biology, agriculture, and microelectronics (Wu et al., 2012; Libralato et al., 2013; Corsi et al., 2014; Libralato, 2014; Minetto et al., 2014). Further applications are currently focused on environmental remediation due to their likely performance in contamination removal and toxicity mitigation (Gavaskar et al., 2005; Tratnyek and Johnson, 2006). Iron-based ENPs stimulated research for engineering applications especially for treating polluted water and groundwater (Tang and Lo, 2013) including both inorganics and organics (Crane and Scott, 2014; Mar Gil-Díaz et al., 2014; Zeino et al., 2014). Their impact is still highly empirical and limited to nanoparticles' elemental composition, size and stability showing both positive and negative effects. The high reactivity of iron-based ENPs, and in particular of nano-zerovalent iron (nZVI), in association with their high specific surface area made them suitable to immobilise and degrade contaminants in soils (Chang et al., 2007; Machado et al., 2013). Thus, the use of nZVI for soil clean-up purposes could pose potential hazards for macrophytes and soil organisms (Ma X. et al., 2010; Ma Y. et al. 2010). In all ecosystems, plants are the basic component playing a crucial role in the fate and transport of ENPs in the environment through plant uptake and bioaccumulation (Monica and Cremonini, 2009).

Although in remediation activities, terrestrial macrophytes could be directly exposed and potentially affected by nZVI, effect data are still scarce despite the current use of this technique (Li et al., 2015). Zhu et al. (2008) found that *Cucurbita maxima* grown in an aqueous medium absorbed, translocated and accumulated Fe_3O_4 ENPs, but this event did not occur with *Phaseolus limensis*

* Corresponding author at: Department of Environmental Sciences, Informatics and Statistics, University Ca' Foscari Venice, Campo della Celestia, 2737/b, I-30122 Castello, Venice, Italy.
E-mail address: giovanni.libralato@unive.it (G. Libralato).

http://dx.doi.org/10.1016/j.ecoenv.2015.07.024
0147-6513/© 2015 Elsevier Inc. All rights reserved.

under the same testing conditions. This suggested that the biological effect could be species-dependent. Lee et al. (2010) showed that Fe_3O_4 ENPs in *Arabidopsis thaliana* did not significantly affect seed germination and the number of produced leaves, while the root elongation was negatively influenced at all exposure concentrations (400, 2000, and 4000 mg Fe_3O_4/L). Kim et al. (2014, 2015) investigated the effect of nZVI on *A. thaliana* root elongation showing an enhanced growth by 150–200% at 0.5 g/L compared to the blank. Further studies on *A. thaliana* evidenced that nZVI triggered high plasma membrane H^+-ATPase activity resulting in a 5-fold higher stomatal opening than in unexposed plants (Kim et al., 2015). Mushtaq (2011) observed that concentrations of Fe_3O_4 ENPs within 100–5000 mg/L were able to significantly reduce *Cucumis sativus* root development compared to controls suggesting the presence of stressing conditions. Phytotoxic effects of Fe_3O_4 ENPs were assessed in lettuce (*Lactuca sativa*), radish (*Raphanus sativus*) and cucumber (*C. sativus*) (Wu et al., 2012) evidencing median effective concentrations (EC50) of more than 5000 mg/L for lettuce and radish, and of 1682 mg/L for cucumber, respectively. For all species, the germination index was significantly different from standard conditions showing seedling inhibition effects. Seeds of *Linum usitatissimum*, *Lolium perenne* and *Hordeum vulgare* were used to investigate the potential inhibition effects of nZVI (El-Temsah and Joner, 2012). Concentration of 2 and 5 g/L of nZVI completely inhibited seed germination, while no detrimental effects on plants were observed at concentrations <250 mg/L. Pereira et al. (2013) observed changes in root and shoot lengths, number of lateral roots, photosynthetic pigments, and internal CO_2 concentration in four rice cultivars when nano-iron exposure in the growth medium increased from 4 to 9 mM. Similarly, other authors found differences in plant growth, nutrient uptake, and lateral roots morphology in *Ipomoea pescaprae* and *Canavalia rosea* when exposed to bulk $FeSO_4$ (Siqueira-Silva et al., 2012). Ma et al. (2013) showed that concentrations higher than 200 mg/L of nZVI reduced plant growth and biomass in *Typha latifolia* and hybrid poplar (*Populous deltoids* × *Populous nigra*). Trujillo-Reyes et al. (2014) investigated the effects of Fe_3O_4 ENPs in *L. sativa*. No physiological change was detected compared to negative controls. Iron ions or ENPs (10 and 20 mg/L) had low or no negative effect on cell membrane integrity and chlorophyll content. Mukherjee et al. (2014) studied ZnO iron doped (Fe@ZnO) ENPs toxicity in *Pisum sativum* (L.) analysing seed germination, uptake, chlorophyll and H_2O_2 content and enzymatic activity. No signs of necrosis, stunting, chlorosis or wilting were found, while variations were observed concerning physiological and biochemical responses in terms of plant growth, chlorophyll content and induction of reactive oxygen species (ROS). Li et al. (2015) observed that *Arachis hypogaea* seeds exposed to nZVI (0.0024 and 0.0048 mg/L) produced significantly longer seedling compared to negative controls suggesting that nanoparticles may have penetrated the peanut seed coat increasing the water uptake and thus stimulating germination.

This short overview indicated that phytotoxicity data about nZVI are still scarce on macrophytes that are key direct biological targets in case of nanoremediation activities, thus, not sufficient for a sound environmental hazard assessment and most data are based just on nominal concentrations. The aim of this research was to understand the potential effect of nZVI compared to its ionic and micro-sized form considering three well-known testing species (*Lepidium sativum*, *Sinapis alba* and *Sorghum saccharatum*) (Baudo, 2012) and four endpoints (germination, seedling elongation, germination index and biomass).

2. Materials and methods

2.1. Materials and reagents

Commercially available materials were purchased for the experiments: $FeCl_3 \cdot 6H_2O$ (iFe) (Sigma-Aldrich, USA), micro-sized iron (mFe) (Aldrich Chemistry, Germany) and nano-sized zerovalent iron (nFe) (American Elements, USA). Boric acid (Sigma-Aldrich, USA) was used as reference toxicant. Concentrated HCl (34–37%, SpA) and HNO_3 (67–69%, SpA) were purchased from Romil. All reagents used during the experiment were of analytical grade.

Stock solutions and suspensions of 10 g/L and all treatments including negative and positive controls were made in ultrapure water (Zeneer Power III Human 18.3 MΩ cm). Suspensions were sonicated for 1 h at 335 W in an ultrasonic bath (3510 MTH, Branson) just after their gravimetric preparation. Treatment solutions and suspensions were aged 72 h and manually shaken for 1 min before starting phytotoxicity tests.

2.2. Primary and secondary characterisation

Particle size distributions (hydrodynamic diameters) and zeta potential of nFe water suspensions were measured on a Zetasizer Nano ZS (Malvern Instruments Ltd., Malvern, UK) equipped with a 633 nm HeNe laser operating at 25 ± 0.1 °C in a back-scattering configuration. The suspensions were analysed immediately after their preparation and after 24 h of ageing. The analytical concentration was achieved by mass spectrometry with inductively coupled plasma source (NexION 300D Perkin-Elmer, ICP-MS). Samples for ICP-MS were treated using EPA Method 3051A (EPA, 2007). Briefly, 0.5 g of solution or suspension was weighed in a Teflon vessel followed by the addition of 9 mL of HNO_3 and 1 mL of HCl. Samples were digested with a microwave system (MARS V CEM) according to the following program: temperature ramp up to 175 °C in 5.5 min and maintaining this temperature for 4.5 min. Once cooled, the samples were transferred to 50 mL polyethylene tubes and brought to a final volume of 50 mL with ultrapure water. The instrumental measurement of the obtained solutions was performed in Dynamic Reaction Cell (DRC) mode using NH_3 as reaction gas and Rh at 10 μg/L was used as internal standard.

Treatments were monitored for pH and Eh at 25 °C to keep germination condition under control ($pH > 5$) (OECD, 2006) and evaluate the abundance and partitioning of Fe ionic species. A solution of NaOH 3 M was used to adjust pH levels of iFe treatments above this threshold.

2.3. Ecotoxicity

Phytoxicity tests were carried out according to Beltrami et al. (1999) and OECD (2006). A battery of three macrophytes was selected including two dicotyledonous (*Lepidium sativum* and *Sinapis alba*) and one monocotyledon (*Sorghum saccharatum*) species (Baudo, 2012). Certified seeds were purchased from Ecotox Ltd. (*L. sativum*-lot LES290311; *S. alba*-lot SIA051011; *S. saccharatum*-lot SOS140611). Germination (%), seedling elongation inhibition (SEI, %), germination index (GI, %) (Beltrami et al., 1999) and inhibition of biomass production normalised to germinated seeds (g, dry weight) were considered as endpoints. All endpoints were assessed in triplicate, otherwise explicitly indicated, including negative (ultrapure water) and positive (H_3BO_3) controls. The common accepted threshold level when ten seeds are exposed per replicate in negative control is $\leq 10\%$ (Beltrami et al., 1999; OECD, 2006). The GI can assume values greater or lower than 100%, where a value equal to 100% means that the seedling average length and germination rate between a specific treatment and the

negative control are exactly the same (Baudo, 2012). If values are between 80% and 120%, the effects are likely the negative controls, otherwise values greater than 120% indicate biostimulation and lower than 80% inhibition effects.

Polystyrene Petri dishes equipped with a Whatman no. 1 filter were used as testing chambers containing 5 mL of treatment solutions (iFe) or suspensions (mFe and nFe). The experimental design assessed 8 treatment solutions for iFe, and 7 suspensions for mFe and nFe. All treatments were geometrically scaled and directly showed in results as real concentrations. Two further suspensions of about 5 and 50 g/L of iFe were considered to check for the effects of nFe concentrations used in nanoremediation activities (Grieger et al., 2010). Ten seeds were incubated per Petri dish for 72 ± 1 h at 25 ± 1 °C in the dark. Results were acquired using a digital camera corrected for objective distortion. The number of germinated seeds was registered and the whole length of seedling measured. Biomass on a dry weight basis was obtained after drying batches of replicated seedlings at 105 ± 1 °C for 24 h (UNE500, Memmert).

2.4. Microscopy

Fresh, unfixed tissues of *L. sativum*, *S. alba* and *S. saccharatum* exposed to nZVI were observed in bright-field mode with a Leica DM750 optical microscope coupled with a Leica ICC50 HD camera. For high magnification optical and electron microscopy of *S. saccharatum*, $1 \times 1\ mm^2$ tissue samples were fixed in 3% glutaraldehyde in 0.1 M cacodylate buffer (CB, pH 7) for 24 h at 4 °C. Samples were washed three times in CB and postfixed with 1% osmium tetroxide in CB for 1 h at 4 °C. Following the removal of secondary fixative, samples were dehydrated in a graded ethanol series and propylene oxide. Epon-812 resin infiltration was carried out from propylene oxide as following mixtures: 5:1 (5 h at 37 °C), 3:1 (5 h at 37 °C), 1:1 (overnight at 37 °C), 1:3 (5 h at 37 °C), and two consecutive times with pure resin overnight at room temperature. Samples were cured increasing the temperature from 37 to 60 °C during 72 h. Semi-thin sections (250 nm to 1 μm thickness) were made with a glass knife on a Leica RM2265 rotary microtome, transferred on glass slides and observed with a Leica DMI 6000 B inverted microscope coupled to a Leica DFC360 FX CCD camera. Ultrathin sections (~60 nm) were made with glass or diamond knifes on RMC Powertome PC ultramicrotome and deposited on 200 mesh copper grids. The grids were stained for 15 min with saturated uranyl acetate in 50% ethanol and 5 min with Reynold's lead citrate. The grids were observed with FEI Tecnai 12 G2 electron microscope operated at 120 kV. Micrographs were recorded on a side-mounted, Olympus Morada CCD camera up to an instrumental magnification of 42000 ×.

2.5. Data analysis

Endpoints' assessment was carried out with ImageJ (Schneider et al., 2012). Whenever possible, toxicity was expressed as EC50 along with 95% confidence limit values with parametric methods such as linear regression. Otherwise, toxicity was expressed as percentage of effect (%) at its relative exposure concentration.

The significance of differences between average effect values of different experimental treatments and controls was assessed by the analysis of variance (ANOVA) considering a significance threshold level always set at 5%. When ANOVA revealed significant differences among treatments, post-hoc tests were carried out with Dunnett's method and Tukey's test. Statistical analyses were performed using Microsoft® Excel 2013/XLSTAT©-Pro (Version 7.2, 2003, Addinsoft, Inc., Brooklyn, NY, USA).

3. Results

3.1. Physico-chemical characterisation of powders, solutions and suspensions

Microscopy analyses of mFe and nFe (Figs. S1 and S2) revealed that primary particle sizes were 59 ± 48 μm and 25 ± 10 nm, respectively. Average hydrodynamic diameter of nFe obtained from DLS in ultrapure water after 10 min of contact time was 289 ± 47 nm between 4.81 and 992 mg/L of nFe. After 24 h of contact time and resuspension by handshaking for 1 min, it was 208 ± 43 nm ($n=7$). Zeta-potential values were all >30 mV for suspensions presenting a concentration greater than 34.33 mg/L.

Total iron determinations by ICP-MS showed the following exposure concentrations: 1.29 ± 0.02, 2.21 ± 0.01, 4.9 ± 0.4, 10.8 ± 0.1, 28.3 ± 0.3, 71.9 ± 0.6, 801 ± 9 and 1750 ± 11 mg/L of iFe; 1.71 ± 0.04, 1.86 ± 0.03, 2.84 ± 0.06, 3.54 ± 0.01, 4.31 ± 0.09, 8.7 ± 0.1 and 10.8 ± 0.3 mg/L of mFe; 4.81 ± 0.03, 34.3 ± 0.4, 116 ± 0.2, 154 ± 0.09, 320 ± 0.3, 875 ± 1, 992 ± 0.8, 2340 ± 27 and 33560 ± 153 mg/L of nFe.

The values of pH (25 ± 1 °C) were naturally between 5 and 6 for mFe and nFe. The pH of iFe treatments were adjusted between 6 and 7 via the addition of NaOH since sub-acidic conditions ($pH > 5$) are required for seed germination and development (OECD, 2006). All redox potentials were slightly positive. According to Beverskog and Puigdomenech (1996), most of the ionic iron was present as Fe^{2+} that is the most bioavailable iron form for plants (Morrissey and Guerinot, 2009; Hasegawa et al., 2011; He et al., 2013) and animals (Benito and Miller, 1998).

3.2. Ecotoxicity

Quality assurance and quality control procedures included both blanks and a reference toxicant (H_3BO_3) for all testing species. Negative controls were always acceptable (effect ≤10% of the germination inhibition). The EC50s of the reference toxicant were 877 (869–885) mg/L, 486 (478–494) mg/L and 980 (972–988) mg/L for *L. sativum*, *S. alba* and *S. saccharatum*, respectively. All values were suitable according to Baudo (2012).

The effects on SEI, GI and biomass production inhibition resulting from the exposure to iFe, mFe and nFe of *L. sativum*, *S. alba* and *S. saccharatum* were summarised in Figs. 1–3, respectively. Toxicity data were not fitted due to the absence of specific effect trends.

3.2.1. Germination inhibition

The species most sensitive to germination was *S. alba* (6% ungerminated seeds) and to a lower extent *L. sativum* (2%) and *S. saccharatum* (2%), respectively. Effects were iFe≅mFe≅nFe for *L. sativum*, iFe≅nFe < mFe for *S. alba*, and mFe < iFe < nFe for *S. saccharatum*. All results were in accordance with negative controls (≤10%).

3.2.2. Seedling elongation inhibition

According to all treatment conditions and biological models considered, it was not possible to determine EC50 values for SEI. Frequently, seed populations provided scattered responses about SEI generating standard deviations exceeding the average effect values. In *L. sativum* (Fig. 1), no significant differences ($p < 0.05$) were observed within mFe and nFe treatments. The ionic iron highest exposure concentration (1570 mg/L) showed effects (41 ± 7%) significantly higher than all other treatments. The maximum detected effects were 1 ± 18% at 8.74 mg/L for mFe and 29 ± 38% at 154 mg/L for nFe. It was noted that biostimulation effects could occur whenever low toxic effects are detected, thus increasing measurements deviations. At 33,560 mg nFe/L,

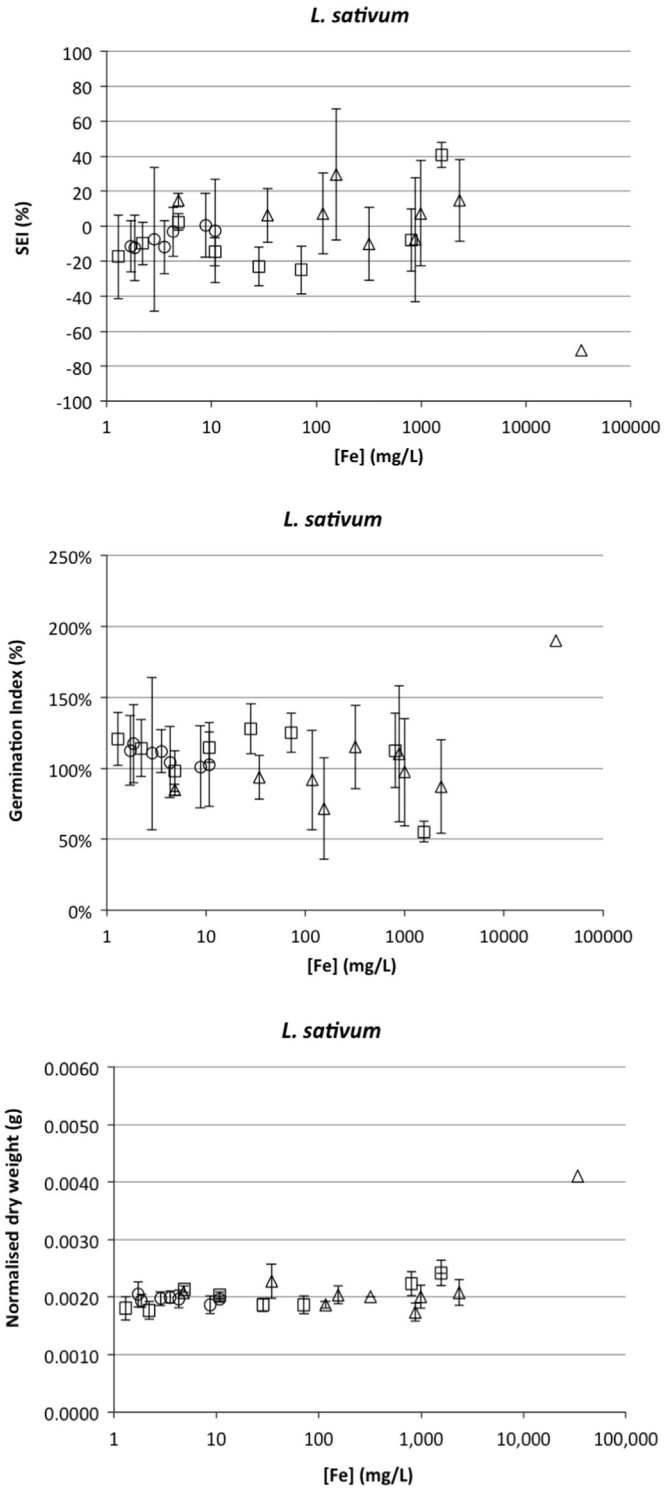

Fig. 1. Effects of iFe (□), mFe (O) and nFe (Δ) on *L. sativum* considering seedling elongation inhibition (SEI, %), germination index (%) and dry weight (g) normalised on the number of germinated seeds.

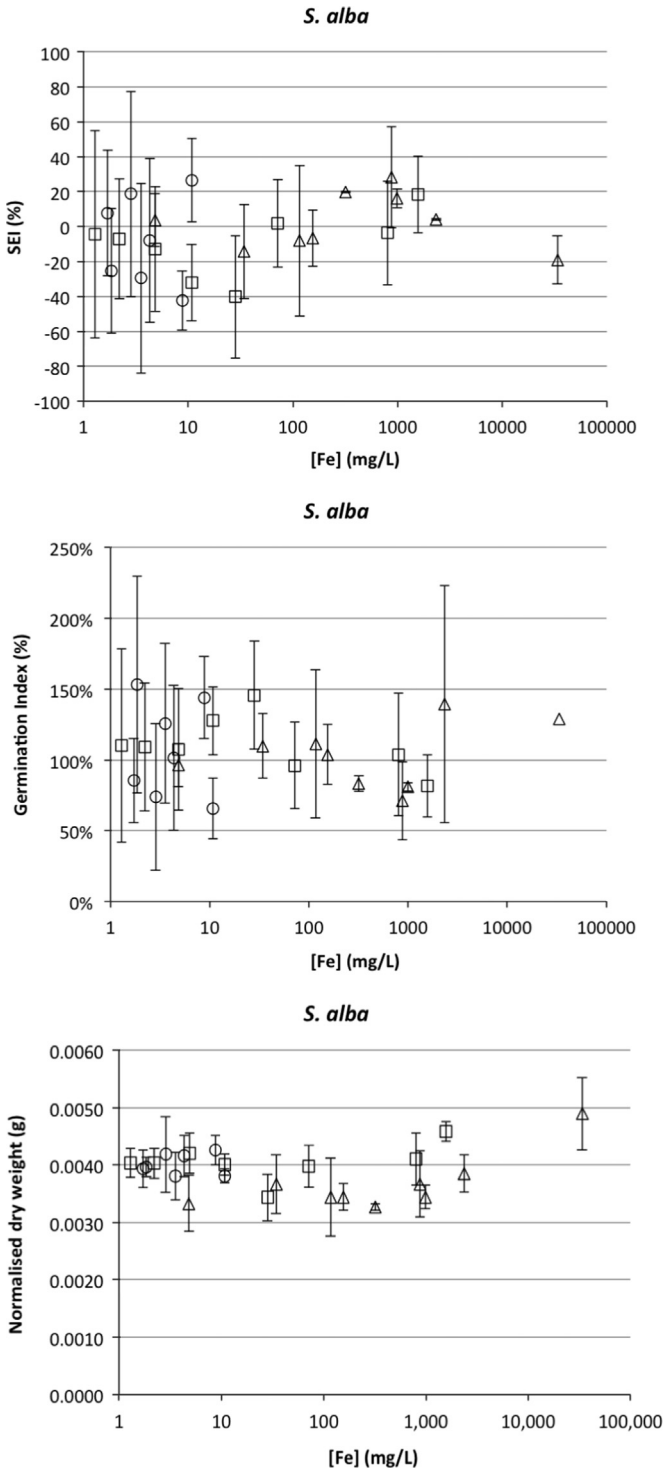

Fig. 2. Effects of iFe (□), mFe (O) and nFe (Δ) on *S. alba* (B) considering seedling elongation inhibition (SEI, %), germination index (%) and dry weight (g) normalised on the number of germinated seeds.

biostimulation was of about 70% ($n=1$). In *S. alba* (Fig. 2), no significant differences ($p<0.05$) were evidenced with iFe, mFe and nFe treatments. Maximum toxic effects were $18\pm22\%$ at 1570 mg/L for iFe, $27\pm24\%$ at 10.78 mg/L for mFe, and $28\pm29\%$ for nFe at 875 mg/L. At 33,560 mg nFe/L, biostimulation was of about $19\pm14\%$ ($n=2$). In *S. saccharatum* (Fig. 3), no significant differences ($p<0.05$) were evidenced amongst treatments for mFe and nFe. For iFe, only the effects at 10.78 mg/L ($-68\pm41\%$) and 1570 mg/L ($45\pm24\%$) were significantly different. At low iFe concentrations, biostimulation effects were detected, whereas at higher ones SEI was shown. All mFe exposure concentrations showed biostimulation effects with a maximum of $59\pm12\%$ at 1.86 mg/L. The maximum toxic effect for nFe was $9\pm27\%$ at 320 mg/L, while at 33,560 mg nFe/L biostimulation was evidenced ($-13\pm36\%$).

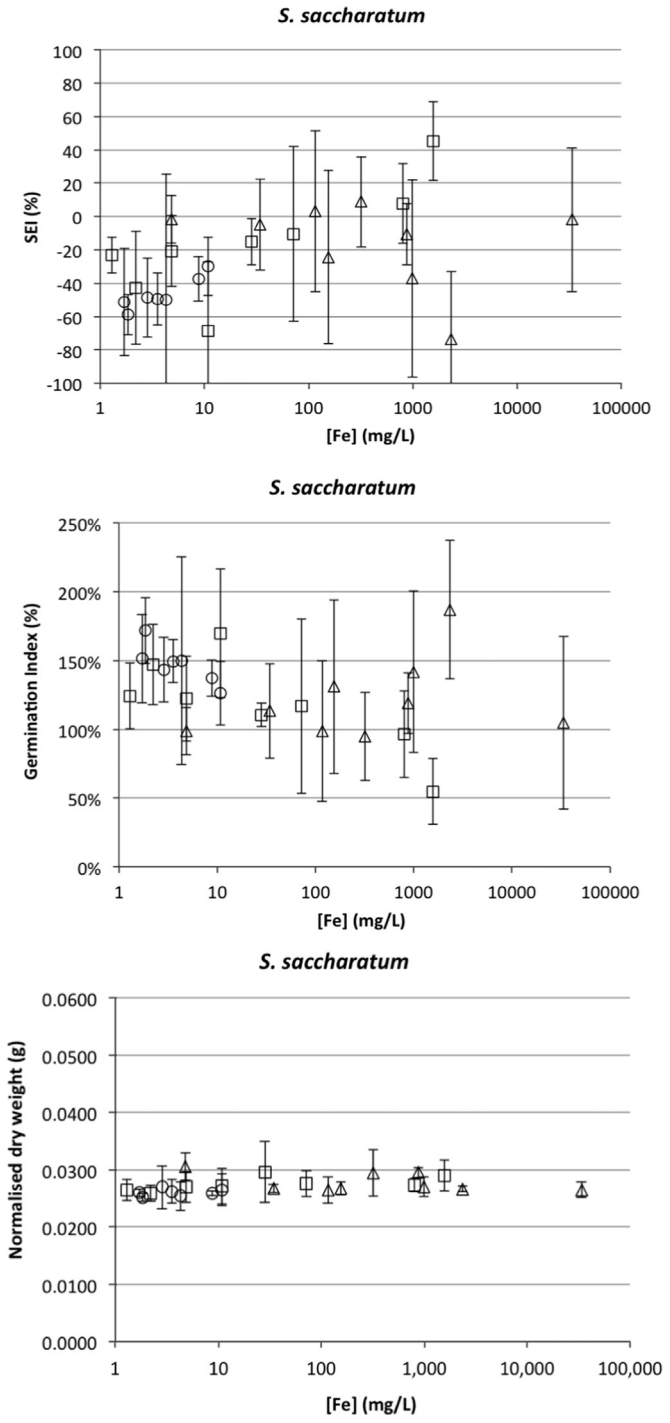

Fig. 3. Effects of iFe (□), mFe (O) and nFe (Δ) on *S. saccharatum* considering seedling elongation inhibition (SEI, %), germination index (%) and dry weight (g) normalised on the number of germinated seeds.

3.2.3. Germination index

In *L. sativum* (Fig. 1), no significant differences ($p < 0.05$) were evidenced amongst treatments for mFe and nFe. Only the ionic iron highest exposure concentration (1570 mg/L) showed a GI significantly different ($55 \pm 7\%$) than all other treatments (98–128%); this is the only exposure presenting adverse effects. The GI values ranged between 101% and 113% for mFe, while between 72% (154 mg/L) and 190% (33,560 mg/L) for nFe. Nevertheless a slight inhibition was found at 154 mg/L of nFe, stimulation effects appeared at greater treatment concentrations. Exposure scenarios suggested the presence of effects not significantly different from the negative controls, apart from biostimulation events associated to nFe highest exposure levels. In *S. alba* (Fig. 2), no significant differences ($p < 0.05$) were evidenced amongst treatments for iFe, mFe and nFe. The GIs varied between 81% and 145% for iFe, 66% and 153% for mFe, and 81% and 139% for nFe. Only for mFe, GI < 80% were observed at 2.84 mg/L ($74 \pm 52\%$) and 10.78 mg/L ($66 \pm 21\%$). All other treatments were likely the negative controls or presented biostimulation effects. At 33,560 mg nFe/L, the GI evidenced the presence of biostimulation (129%), while the highest value of GI was obtained at 2340 mg nFe/L. In *S. saccharatum* (Fig. 3), no significant differences ($p < 0.05$) were evidenced amongst treatments for mFe and nFe. For iFe, only GIs at 10.78 mg/L ($170 \pm 47\%$) and 1570 mg/L ($55 \pm 24\%$) were significantly different showing inhibitory effects. GI levels ranged between 55% and 170% for iFe, 126% and 172% for mFe, and 95% and 187% for nFe. At 33,560 mg nFe/L, the GI evidenced the presence of biostimulation ($105 \pm 63\%$), while the highest value of GI ($187 \pm 50\%$) was obtained at 2340 mg nFe/L. Generally, the GI outputs were less variable compared to SEI due to the combination of germination and SEI data.

3.2.4. Biomass

The biomass normalised on germinated seeds in *L. sativum* (Fig. 1) evidenced no significant differences ($p < 0.05$) amongst treatments and between treatments and negative controls for iFe, mFe and nFe except for the highest nFe concentrations. At 33,560 mg nFe/L, the generated biomass was significantly different ($p < 0.001$) from both negative controls and treatments being more than double. The mean biomass value was 0.0021 ± 0.0004 g. In *S. alba* (Fig. 2), no significant differences ($p < 0.05$) were evidenced amongst treatments and between treatments and negative controls for iFe, mFe and nFe apart from the following specific exposure conditions. At 33,560 mg nFe/L, the generated biomass was significantly different ($p < 0.01$) from both negative controls and treatments being about 25% greater. At 28.29 mg iFe/L, the biomass was significantly different ($p < 0.01$) from the one of negative controls and 1570 mg iFe/L being about 25% lower. The mean biomass value was 0.0039 ± 0.0004 g. In *S. saccharatum* (Fig. 3), no significant differences were evidenced amongst treatments and between treatments and negative controls for iFe, mFe and nFe presenting a mean value of 0.0273 ± 0.0015 g.

A great variability in SEI and to a lower extent in GI data was observed for all testing species in all replicated experiments. Only biomass data presented average coefficients of variation < 20% (19%, 10% and 5% for *L. sativum*, *S. alba* and *S. saccharatum*, respectively). Thus, SEI and GI cannot be deemed as suitable endpoints for the considered species and targeted substances, especially for mFe and nFe. Conversely, the inhibition of the biomass normalised to the number of germinated seeds (i.e. the same seedlings used for SEI and GI) could be considered as an appropriate endpoint.

3.3. Microscopy

Bright-field optical microscopy observations were reported in Fig. 4 for *L. sativum*, *S. alba* and *S. saccharatum* exposed at 992 mg nFe/L for 72 h at 25 °C. Fig. S3 shows representative images of leaf, shoot and root sections of *S. saccharatum* exposed at 992 mg nFe/L for 72 h at 25 °C. In *L. sativum*, *S. alba* and *S. saccharatum* roots (Fig. 4), black spots probably made of ferric hydroxides and nZVI aggregates were present at most treatment concentrations as in Ma et al. (2013). Sometimes, they assumed the shape of a coating, like in Ma et al. (2013), especially at 2340 and 33,560 mg/L of nFe. Probably, the test duration influenced the coating formation being not a medium-term exposure (i.e. 4 weeks), but a short-term one

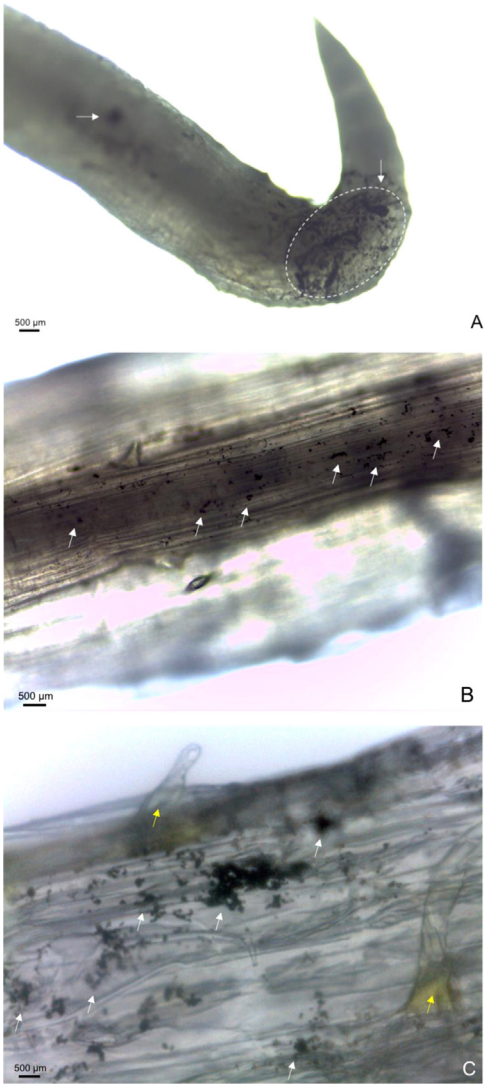

Fig. 4. Bright-field micrographs illustrating root apex of *L. sativum* (A) and root longitudinal sections of *S. alba* (B) and *S. saccharatum* (C) treated with 992 mg/L of nFe for 72 h at 25 °C. White arrows indicate nFe aggregates, while yellow ones root hairs. (For interpretation of the references to color in this figure legend, the reader is referred to the web version of this article.)

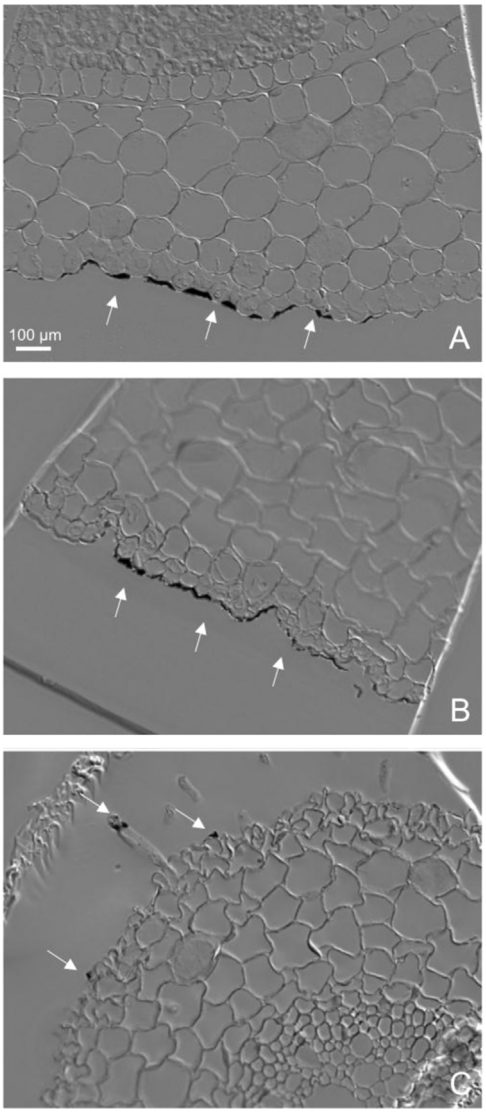

Fig. 5. DIC images of unstained, transverse sections of leaf (A), shoot (B) and root (C) of *S. saccharatum* treated with 992 mg/L of nFe for 72 h at 25 °C. White arrows indicate the presence of nFe deposits/agglomerates/precipitates.

(72 h). No black spots were found after the exposure to iFe or mFe treatments. Root longitudinal sections indicated for both *S. alba* (Fig. 4B) and *S. saccharatum* (Fig. 4C) the presence of nZVI aggregates, apparently, inside the tissues. In Fig. 5, the transverse section of *S. saccharatum* leaf, shoot and root showed that nFe did not enter palisade cells or xylem (tracheids and parenchyma cells) remaining on their outer parts. The same was confirmed by TEM (Fig. S4). All nFe aggregates were located outside the cell walls. We found three main possible co-existing explanations for these findings: (a) ENPs entered the root and started to be transported upward to the shoot forming some aggregates; (b) ENPs were formed inside the root tissues precipitating Fe^{2+}/Fe^{3+}; and (c) the presence of ENPs was the results of a false positive due to sample preparation. The debate about the mode of uptake of metallic ENPs is still open as well as the mechanism of NPs formation within plants (Taylor et al., 2014). About silver, *Brassica juncea* and *Medicago sativa* roots took up ions that were transformed into Ag NPs within the plant (Harris and Bali, 2008). Some Au NPs appeared to be able to move through the transpiration stream up to the aerial tissues (Taylor et al., 2014) as well as transported via xylem and phloem such as for CuO NPs (Wang et al., 2012). Other authors evidenced the potential translocation of fullerenes (Lin et al., 2009), CeO_2 (Hong et al., 2014) and nZVI (Ma et al., 2013) in macrophytes. Kim et al. (2014, 2015) suggested that when *A. thaliana* seeds are treated with nZVI the induced OH radicals may thin or open plant seed coat and, thus, Li et al. (2015) suspected that nZVI could penetrate *A. hypogaea* seed coat increasing water uptake promoting seedling development.

Further investigations will be necessary to understand the ability of ENPs to directly enter plant tissues and xylem and their translocation mechanisms to shoot and leaves. At the same time, it will be important to strengthen the way samples for microscopy are prepared in order to assure that false positives are avoided.

4. Generalised discussion

Results from all endpoints evidenced that nZVI at concentrations used for field activities (2340 and 33,560 mg/L) was not phytotoxic. Germination, SEI, GI and biomass did not show significant toxic effects compared to negative controls with no apparent difference in the sensitivities between dicotyledons (*L. sativum* and *S. alba*) and monocotyledon (*S. saccharatum*),

nevertheless the high variability of SEI data. Conversely, biostimulation phenomena frequently occurred at higher mFe and nFe levels suggesting that iron is present in a more bioavailable form than iFe at concentrations suitable to act as micro-nutrients like reported by Li et al. (2015).

The pH and Eh of nFe suspensions after 72 h exposure to biological models (pH=6.65 and Eh=0.024 V for *L. sativum*; pH=7.18 and Eh=−0.006 V for *S. alba*; pH=6.61 and Eh=0.026 V for *S. saccharatum*) still indicated the presence of Fe^{2+} according to Beverskog and Puigdomenech (1996). This is in contrast with Ma et al. (2013) results that evidenced a drastic reduction in *T. latifolia* weight and shoot height after four weeks of exposure to nZVI at 1 g/L, and El-Temsah and Joner (2012) that showed a complete germination inhibition at 1000–2000 mg/L of nZVI (nominal concentrations) for *L. usitatissimum*, *L. perenne* and *H. vulgare*. Actually, concentrated nZVI suspensions showed high aggregation rates that reduced the reaction surface decreasing as well their efficiency and effects (Diao and Yao, 2009). Adverse effects on SEI and GI were shown at 1570 mg iFe/L, but they did not affect the production of biomass that was not significantly different from the respective negative controls.

5. Conclusions

According to the considered standard endpoints (inhibition of germination, seedling elongation, and biomass production and germination index) and experimental scenarios, ionic iron, and micro- and nano-sized iron particles showed no significant adverse effects to *L. sativum*, *S. alba* and *S. saccharatum*. Neither nZVI field exposure concentrations (2340 ± 27 mg/L and $33{,}560 \pm 153$ mg/L) evidenced adverse effects significantly different from negative controls. Moderate biostimulation was observed at the most concentrated treatments especially for micro- and nano-sized iron. The exposure of nZVI to *S. saccharatum* highlighted potential uptake phenomena and macroscopic findings such as black spots and coatings in roots. Further investigations are necessary to understand their nature (i.e. nano- or micro-sized composition) as well as the uptake mechanisms and the potentiality for species-specific effects. The safety of nZVI should be ascertained also with medium- and long-term exposure assays to check if an excess of nZVI may compete with other essential elements limiting their bioavailability and causing stress phenomena to the target organisms.

Appendix A. Supplementary material

Supplementary data associated with this article can be found in the online version at http://dx.doi.org/10.1016/j.ecoenv.2015.07.024.

References

Baudo, R., 2012. Report on the International Interlaboratory Comparison on the Phytotoxkit, pp. 1–115.

Beltrami, M., Rossi, D., Baudo, R., 1999. Phytotoxicity assessment of Lake Orta sediments. Aquat. Ecosyst. Health 2, 391–401. http://dx.doi.org/10.1080/14634989908656977.

Benito, P., Miller, D., 1998. Iron absorption and bioavailability: an updated review. Nutr. Res. 18, 581–603.

Beverskog, B., Puigdomenech, I., 1996. Revised Pourbaix diagrams for iron at 25–300 °C. Corros. Sci. 28, 29–43.

Chang, M.C., Shu, H.Y., Hsieh, W.P., Wang, M.C., 2007. Remediation of soil contaminated with pyrene using ground nanoscale zero-valent iron. J. Air Waste Manag. Assoc. 57, 221–227.

Corsi, I., Cherr, G.N., Lenihan, H.S., Labille, J., Hasselov, M., Canesi, L., Dondero, F., Frenzilli, G., Hristozov, D., Puntes, V., Libralato, G., Marcomini, A., Sabbioni, E., Matranga, V., 2014. Common strategies and technologies for the ecosafety assessment and design of nanomaterials entering the marine environment. ACS Nano 8, 9694–9709. http://dx.doi.org/10.1021/nn504684k.

Crane, R.A., Scott, T.B., 2014. The removal of uranium onto nanoscale zero-valent iron particles in anoxic batch systems. J. Nanomater., 956360. http://dx.doi.org/10.1155/2014/956360.

Diao, M., Yao, M., 2009. Use of zero-valent iron nanoparticles in inactivating microbes. Water Res. 43, 5243–5251. http://dx.doi.org/10.1016/j.watres.2009.08.051.

El-Temsah, Y.S., Joner, E.J., 2012. Impact of Fe and Ag nanoparticles on seed germination and differences in bioavailability during exposure in aqueous suspension and soil. Environ. Toxicol. 27, 42–49. http://dx.doi.org/10.1002/tox.20610.

EPA, 2007. Microwave assisted acid digestion of sediments, sludges, soils and oils Method 3051A.

Gavaskar, A., Tatar, L., Condit, W., 2005. Cost and Performance Report: Nanoscale Zero-Valent Iron Technologies for Source Remediation.

Grieger, K.D., Fjordbøge, A., Hartmann, N.B., Eriksson, E., Bjerg, P.L., Baun, A., 2010. Environmental benefits and risks of zero-valent iron nanoparticles (nZVI) for *in situ* remediation: risk mitigation or trade-off? J. Contam. Hydrol. 118, 165–183.

Harris, A., Bali, R., 2008. On the formation and entent of uptake of silver nanoparticles by live plants. J. Nanopart. Res. 10, 691–695.

Hasegawa, H., Rahman, A.M., Saitou, K., Kobayashi, M., Okumura, C., 2011. Influence of chelating ligands on bioavailability and mobility of iron in plant growth media and their effect on radish growth. Environ. Exp. Botany 71, 345–351.

He, W., Shohag, M.J.I., Wei, Y., Feng, Y., Yang, X., 2013. Iron concentration, bioavailability, and nutritional quality of polished rice affected by different forms of foliar iron fertilizer. Food Chem. 141, 4122–4126.

Hong, J., Peralta-Videa, J.R., Rico, C., Sahi, S., Viveros, M.N., Bartonjo, J., Zhao, L., Gardea-Torresdey, J.L., 2014. Evidence of translocation and physiological impact of foliar applied CeO_2 nanoparticles on cucumber (*Cucumis sativus*) plants. Environ. Sci. Technol. 48, 4376–4385.

Kim, J.H., Lee, Y., Kim, E.J., Gu, S., Sohn, E.J., Seo, Y.S., An, H.J., Chang, Y.S., 2014. Exposure of iron nanoparticles to Arabidopsis thaliana enhances root elongation by triggering cell wall loosening. Environ. Sci. Technol. 48, 3477–3485. http://dx.doi.org/10.1021/es4043462.

Kim, J.H., Oh, Y., Yoon, H., Hwang, I., Chang, Y.S., 2015. Iron nanoparticle-induced activation of plasma membrane H(+)-ATPase promotes stomatal opening in Arabidopsis thaliana. Environ. Sci. Technol. 4, 1113–1119. http://dx.doi.org/10.1021/es504375t.

Lee, C.W., Mahendra, S., Zodrow, K., Li, D., Tsai, Y.C., Braam, J., Alvarez, P.J., 2010. Developmental phytotoxicity of metal oxide nanoparticles to *Arabidopsis thaliana*. Environ. Toxicol. Chem. 29, 669–675.

Li, X., Yang, Y., Gao, B., Zhang, M., 2015. Stimulation of peanut seedling development and growth by zero-valent iron nanoparticles at low concentrations. Plos One 10, e0122884. http://dx.doi.org/10.1371/journal.pone.0122884.

Libralato, G., 2014. The case of *Artemia* spp. in nanoecotoxicology. Marine Environmental Research 101, 38–43. http://dx.doi.org/10.1016/j.marenvres.2014.08.002.

Libralato, G., Minetto, D., Totaro, S., Mičetić, I., Pigozzo, A., Sabbioni, E., Marcomini, A., Volpi Ghirardini, A., 2013. Embryotoxicity of TiO_2 nanoparticles to *Mytilus galloprovincialis* (Lmk). Mar. Environ. Res. 92, 71–78. http://dx.doi.org/10.1016/j.marenvres.2013.08.015.

Lin, S., Reppert, J., Hu, Q., Hudson, J.S., Reid, M.L., Ratnikova, T.A., Apparao, M.R., Hong, L., Pu, C.K., 2009. Uptake, translocation and transmission of carbon nanomaterials in rice plants. Small 5, 1128–1132.

Ma, Y., Kuang, L., He, X., Bai, W., Ding, Y., Zhang, Z., Zhao, Y., Chai, Z., 2010a. Effects of rare earth oxide nanoparticles on root elongation of plants. Chemosphere 78, 273–279. http://dx.doi.org/10.1016/j.chemosphere.2009.10.050.

Ma, X., Geiser-Lee, J., Deng, Y., Kolmakov, A., 2010b. Interactions between engineered nanoparticles (ENPs) and plants: Phytotoxicity, uptake and accumulation. Sci. Total Environ. 408, 3053–3061.

Ma, X., Gurung, A., Deng, Y., 2013. Phytotoxicity and uptake of nanoscale zero-valent iron (nZVI) by two plant species. Sci. Total. Environ. 443, 844–849. http://dx.doi.org/10.1016/j.scitotenv.2012.11.073.

Machado, S., Stawińskib, W., Sloninab, P., Pintoa, A.R., Grossoa, J.P., Nouwsa., H.P.A., Albergaria, J.T., Delerue-Matosa, C., 2013. Application of green zero-valent iron nanoparticles to the remediation of soils contaminated with ibuprofen. Sci. Total Envion. 461–462, 323–329.

Mar Gil-Díaz, M., Pérez-Sanz, A., Vicente, M.A., Lobo, M.C., 2014. Immobilisation of Pb and Zn in soils using stabilised zero-valent iron nanoparticles: effects on soil properties. CLEAN 42, 1776–1784.

Minetto, D., Libralato, G., Volpi Ghirardini, A., 2014. Ecotoxicity of engineered TiO_2 nanoparticles to saltwater organisms: an overview. Environ. Int. 66, 18–27. http://dx.doi.org/10.1016/j.envint.2014.01.012.

Monica, R.C., Cremonini, R., 2009. Nanoparticles and higher plants. Caryologia 62, 161–165.

Morrissey, J., Guerinot, M.L., 2009. Iron uptake and transport in plants: the good, the bad, and the ionome. Chem. Rev. 109, 4553–4567.

Mukherjee, A., Pokhrel, S., Bandyopadhyay, S., Mädler, L., Peralta-Videa, J.R., Gardea-Torresdey, J.L., 2014. A soil mediated phyto-toxicological study of iron doped zinc oxide nanoparticles (Fe at ZnO) in green peas (*Pisum sativum* L.). Chem. Eng. J. 258, 394–401.

Mushtaq, Y.K., 2011. Effect of nanoscale Fe_3O_4, TiO_2 and carbon particles on cucumber seed germination. J. Environ. Sci. Health. Part A, Tox. Hazard Subst. Environ. Eng. 46, 1732–1735.

OECD, 2006. Guidelines for the Testing of Chemicals, Terrestrial Plant Test Seedling Emergence and Seedling Growth Test.
Pereira, E.G., Oliva, M.A., Rosado-Souza, L., Mendes, G.C., Colares, D.S., Stopato, C.H., Almeida, A.M., 2013. Iron excess affects rice photosynthesis through stomatal and non-stomatal limitations. Plant Sci. 201–202, 81–92. http://dx.doi.org/10.1016/j.plantsci.2012.12.003.
Schneider, C.A., Rasband, W.S., Eliceiri, K.W., 2012. NIH image to ImageJ: 25 years of image analysis. Nat. Methods 9, 671–675.
Siqueira-Silva, A.I., da Silva, L.C., Azevedo, A.A., Oliva, M.A., 2012. Iron plaque formation and morphoanatomy of roots from species of restinga subjected to excess iron. Ecotoxicol. Environ. Saf. 78, 265–275. http://dx.doi.org/10.1016/j.ecoenv.2011.11.030.
Tang, S.C.N., Lo, I.M.C., 2013. Magnetic nanoparticles: essential factors for sustainable environmental applications. Water Res. 47, 2613–2632. http://dx.doi.org/10.1016/j.watres.2013.02.039.
Taylor, A.F., Rylott, E.L., Anderson, C.W.N., Bruce, N.C., 2014. Investigation the toxicity, uptake, nanoparticle formation and genetic response of plants to gold. Plos One 9, e93793.
Tratnyek, P.G., Johnson, R.L., 2006. Nanotechnologies for environmental cleanup. Nano Today 1, 44–48. http://dx.doi.org/10.1016/S1748-0132(06)70048-2.
Trujillo-Reyes, J., Majumdar, S., Botez, C.E., Peralta-Videa, J.R., Gardea-Torresdey, J.L., 2014. Exposure studies of core-shell Fe/Fe3O4 and Cu/CuO NPs to lettuce (Lactuca sativa) plants: Are they a potential physiological and nutritional hazard? J. Hazard Mater. 267, 255–263. http://dx.doi.org/10.1016/j.jhazmat.2013.11.067.
Wang, Z., Xie, X., Zhao, J., Liu, X., Feng, W., White, J.C., Xing, B., 2012. Xylem- and phloem-based transport of CuO nanoparticles in maize (*Zea mays* L.). Environ. Sci. Technol. 46, 4434–4441.
Wu, S.G., Huang, L., Head, J., Chen, D.R., Kong, I.C., Tang, Y.J., 2012. Phytotoxicity of metal oxide nanoparticles is related to both dissolved metals ions and adsorption of particles on seed surfaces. J. Pet. Environ. Biotechnol. 3, 1–6. http://dx.doi.org/10.4172/2157-7463.1000126.
Zeino, A., Abulkibash, A., Khaled, M., Atieh, M., 2014. Bromate removal from water using doped iron nanoparticles on multiwalled carbon nanotubes (CNTS). Journal of Nanomaterials 2.
Zhu, H., Han, J., Xiao, J.Q., Jin, Y., 2008. Uptake, translocation, and accumulation of manufactured iron oxide nanoparticles by pumpkin plants. J. Environ. Monit. 10, 713–717. http://dx.doi.org/10.1039/B805998E.